GEOLOGICAL SURVEY OF CANADA
OPEN FILE 7852

Targeted Geoscience Initiative 4: Contributions to the Understanding of Precambrian Lode Gold Deposits and Implications for Exploration

Geology of the banded iron formation-hosted Meadowbank gold deposit, Churchill Province, Nunavut

Vivien Janvier[1], Sébastien Castonguay[2], Patrick Mercier-Langevin[2], Benoît Dubé[2], Michel Malo[1], Vicki J. McNicoll[3], Robert A. Creaser[4], Benoît de Chavigny[5], and Sally J. Pehrsson[3]

[1]Institut national de la recherche scientifique – Centre Eau Terre Environnement, Québec, Quebec
[2]Geological Survey of Canada, Québec, Quebec
[3]Geological Survey of Canada, Ottawa, Ontario
[4]University of Alberta, Edmonton, Alberta
[5]Agnico-Eagle Mines Ltd., Ottawa, Baker Lake, Nunavut

2015

Recommended citation

Janvier, V., Castonguay, S., Mercier-Langevin, P., Dubé, B., Malo, M., McNicoll, V.J., Creaser, R.A., de Chavigny, B., and Pehrsson, S.J., 2015. Geology of the banded iron formation-hosted Meadowbank gold deposit, Churchill Province, Nunavut, *In:* Targeted Geoscience Initiative 4: Contributions to the Understanding of Precambrian Lode Gold Deposits and Implications for Exploration, (ed.) B. Dubé and P. Mercier-Langevin; Geological Survey of Canada, Open File 7852, p. 255–269.

Contribution to the Geological Survey of Canada's Targeted Geoscience Initiative 4 (TGI-4) Program (2010–2015)

TABLE OF CONTENTS

Geology of the banded iron formation-hosted Meadowbank gold deposit, Churchill Province, Nunavut

Vivien Janvier[1]*, Sébastien Castonguay[2]†, Patrick Mercier-Langevin[2], Benoît Dubé[2], Michel Malo[1], Vicki J. McNicoll[3], Robert A. Creaser[4], Benoît de Chavigny[5], and Sally J. Pehrsson[3]

[1]Institut national de la recherche scientifique – Centre Eau Terre Environnement, 490 rue de la Couronne, Québec, Quebec G1K 9A9
[2]Geological Survey of Canada, 490 rue de la Couronne, Québec, Quebec G1K 9A9
[3]Geological Survey of Canada, 601 Booth Street, Ottawa, Ontario K1A 0E8
[4]University of Alberta, 116 Street and 85 Avenue, Edmonton, Alberta T6G 2R3
[5]Agnico-Eagle Mines ltd, Meadowbank Division, P.O. Box 540, Baker Lake, Nunavut X0C 0A0
*Corresponding author's e-mail: vivien.janvier@ete.inrs.ca
†Corresponding author's e-mail: sebastien.castonguay@RNCan-NRCan.gc.ca

ABSTRACT

The Meadowbank gold deposit is hosted in ca. 2711 Ma banded iron formation (BIF) successions within the polydeformed and metamorphosed Woodburn Lake Group. This volcano-sedimentary sequence comprises several similar BIF successions of which only one contains economical gold mineralization. Deposit host rocks consist of greenschist- to amphibolite-facies, intermediate to felsic volcaniclastic rocks, mafic and ultramafic rocks, quartzite and BIF. Notwithstanding cryptic and strongly overprinted Archean tectonism, four phases of Proterozoic Trans-Hudsonian deformation have been regionally documented. In the Meadowbank deposit area, several generations of structures are recognized: 1) isoclinal F_1 folds and D_1 faults strongly overprinted by 2) south-trending isoclinal F_{2a} folds and associated D_2 fault zones that cut mineralized zones. Late D_2 deformation consists of north-trending gentle F_{2b} folds, 3) open to closed south-west-plunging megascopic F_3 folds, and 4) south-verging shallowly to moderately inclined, open to tight, chevron-style F_4 folds.

The bulk of the gold is hosted in BIF and is associated with pyrrhotite ±pyrite and traces of chalcopyrite and arsenopyrite. Gold-rich quartz-pyrrhotite ±pyrite veins cut intercalated intermediate to felsic volcaniclastic rocks. The ore-associated mineral assemblage includes grunerite and chlorite within BIF, whereas muscovite, chlorite, and pyrite represent the dominant mineral assemblage of altered volcaniclastic rocks. Biotite, Fe-Mg amphibole, and garnet occur in variable modal abundance in the southern part of the deposit, where metamorphic grade is higher.

Crosscutting relationships suggest that most of the gold was preferentially introduced along D_1 faults and was likely remobilized during D_2 deformation, especially along sheared contacts and F_{2a} fold limbs. Deposit- and regional-scale lithogeochemistry coupled with new U-Pb zircon ages indicate that the Meadowbank deposit is located at or near the boundary between two distinct lithological assemblages (2711 Ma and 2717 Ma), which are separated by long-lived fault zones that potentially controlled the occurrence and geometry of the Meadowbank deposit.

INTRODUCTION

The Meadowbank Mine, owned and operated by Agnico Eagle Mines Ltd., is located approximately 70 km north of the community of Baker Lake (Fig. 1a). Approximately 4.2 million ounces of gold, including 1.3 Moz produced from 2010 to 2013, 1.8 Moz in reserve, and 1.2 Moz in resources are comprised in the Portage-Goose and Vault deposits (Agnico Eagle Mines website end of December 2014). Most of the gold is hosted in banded magnetite-chert iron formations, but a significant amount of gold is also associated with quartz veins that cut intercalated intermediate to felsic volcaniclastic rocks. The mineralized succession is part of the polydeformed and metamorphosed Neoarchean Woodburn Lake Group (Sherlock et al., 2004).

In the Meadowbank mine area, the Woodburn Lake Group comprises several major banded iron formations (BIF), including the East BIF, the Central BIF, and the West BIF (Fig. 1b). Despite their mineralogical and textural similarities (e.g. Gourcerol et al., 2014, 2015), only the Central BIF contains economic gold concentration (Portage-Goose deposit), suggesting that key elements and ore-forming processes were specific to that particular BIF interval. Establishing the nature of these key ore-forming event(s) at Meadowbank could

Janvier, V., Castonguay, S., Mercier-Langevin, P., Dubé, B., Malo, M., McNicoll, V.J., Creaser, R.A., de Chavigny, B., and Pehrsson, S.J., 2015. Geology of the banded iron formation-hosted Meadowbank gold deposit, Churchill Province, Nunavut, *In:* Targeted Geoscience Initiative 4: Contributions to the Understanding of Precambrian Lode Gold Deposits and Implications for Exploration, (ed.) B. Dubé and P. Mercier-Langevin; Geological Survey of Canada, Open File 7852, p. 255–269.

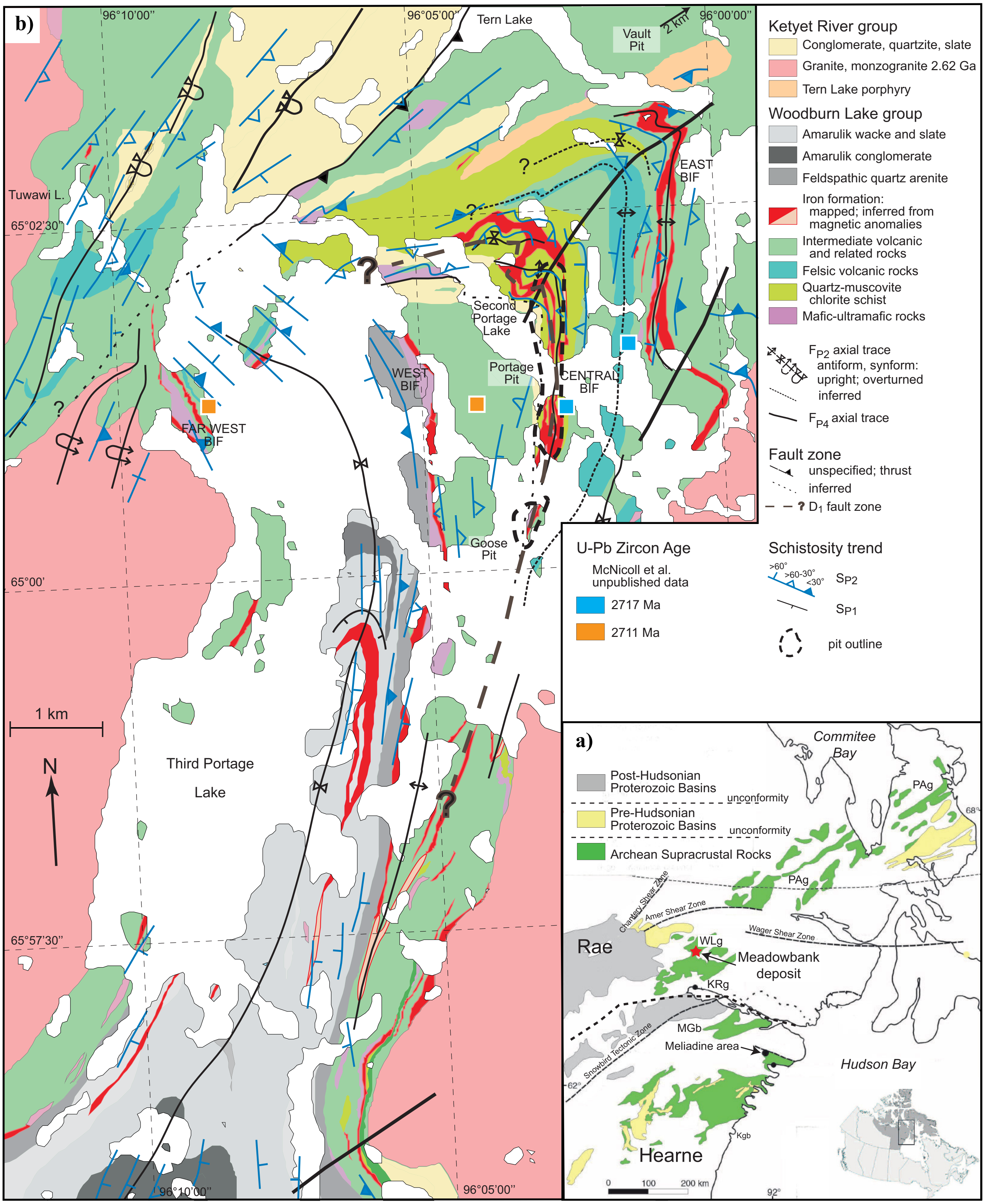

Figure 1. a) Geology and structure of the Meadowbank gold deposit area (modified map and structural nomenclature of Pehrsson et al., 2013). **b)** Simplified geological map of the western Churchill Province (modified from Hrabi et al., 2003). Abbreviations: KGb = Kaminak greenstone belt; KRg = Ketyet River Group; MGb = MacQuoid-Gibson belt; PAg = Prince Albert Group; WLg = Woodburn Lake Group. U-Pb ages from Davis and Zaleski (1998) and McNicoll et al. (unpublished data).

have a major impact on exploration models as well as genetic models for other BIF-hosted gold deposits.

Our field-based research includes geological mapping of the open-pit deposit, detailed description of several drillhole sections, and geochemical characterization of host rocks and their alteration (Castonguay et al., 2012, 2013; Janvier et al., 2013). Geochronology of key units in and around the deposit (Castonguay et al., 2013) and a study of the Vault gold deposit, 10 km north of Portage-Goose deposit (Dupuis et al., 2014), were also undertaken. The present report synthesizes the main geological features of the Portage deposit.

GEOLOGICAL SETTING

The Meadowbank deposit is situated within the Rae domain of the western Churchill Province (Fig. 1a). The Rae domain is dominated by Meso- to Neoarchean granodioritic-tonalitic orthogneiss and supracrustal rocks (Hoffman, 1989; Zaleski et al., 1997, 1999b; Skulski et al., 2003; Berman et al., 2005). The Meadowbank deposit is hosted by the 2.71 Ga Pipedream-Third Portage sequence, the third of five assemblages comprising the ca. 2.73–2.68 Ga Woodburn Lake Group (Fig. 1b; Henderson et al., 1991; Zaleski et al., 1997, 2001; Pehrsson et al., 2013). The Woodburn Lake Group constitutes part of a greenstone belt including greenschist- to amphibolite-facies, ultramafic to mafic volcanic rocks, intermediate volcanic rocks, BIF, quartzite, and oligomictic conglomerate, overlain by Paleoproterozoic (2.3–1.9 Ga) sedimentary rocks of the Ketyet River Group.

Rocks comprising the Woodburn Lake Group in the Meadowbank mine area were likely deformed during the Archean (Ashton, 1988; Zaleski et al., 1999a, 2003; Berman et al., 2005, 2007). However, Archean fabrics are mainly cryptic in the Meadowbank area. Proterozoic reworking, concomitant with the Trans-Hudson Orogeny (1.9–1.8 Ga), is extensive and developed during at least four phases (Hrabi et al., 2003; Sherlock et al., 2004; Pehrsson et al., 2004, 2013; Fig. 1b). The first two Proterozoic deformation phases/increments [D_{P1} and D_{P2}; following Pehrsson et al. (2013), in which the subscript P is used to identify deformation phases of Proterozoic age] are characterized by tight to isoclinal folds. In areas less affected by younger deformation, F_{P1} and F_{P2} folds verge to the south and northwest, respectively. In areas of strong D_{P2} strain or along long limbs of F_{P2} folds, the S_{P1} and S_{P2} axial-planar foliations become generally coplanar, and are thus difficult to differentiate and are often described as a composite S_{P1-2} fabric (Pehrsson et al., 2013). Fault zones associated with these two major episodes of deformation have an impact on the distribution and geometry of ore zones, which will be discussed below. The third Proterozoic deformation (D_{P3}) comprises shallowly to moderately north- to northwest-inclined, open to tight, chevron-style mesoscopic folds, locally marked by an axial-planar S_{P3} crenulation cleavage. The D_{P4} regional deformation consists of megascopic upright southeast- or northeast-plunging chevron folds (Fig. 1b).

DEPOSIT HOST ROCKS

The Meadowbank deposit comprises several variably altered, intensely deformed and metamorphosed rock units (Sherlock et al., 2001a). From east to west, rock units consist of intermediate volcaniclastic rocks (unit 1), intermediate to felsic (unit 2) and felsic (unit 3) volcaniclastic rocks intercalated with BIF, mafic volcanic rocks (unit 4), ultramafic rocks (unit 5) and quartzite with mafic (unit 6) to intermediate volcanic rocks (unit 7; Sherlock et al., 2001a; Fig. 2). Unit 1 consists of massive intermediate volcaniclastic rocks that form the structural footwall at the Meadowbank deposit. Volcaniclastic rocks comprise quartz and plagioclase grains within a groundmass of fine-grained quartz, plagioclase, and biotite. Unit 2 comprises medium- to fine-grained, intermediate to felsic volcaniclastic rocks, commonly intercalated with BIF, and quartz ±plagioclase with a significant amount of muscovite and chlorite. Unit 3 is characterized by felsic volcaniclastic rocks, commonly muscovite-altered and intensely foliated, forming distinct muscovite schists. BIF comprises millimetre- to centimetre-thick magnetite and chert layers (1 mm to 3 cm) along with lesser grunerite/cummingtonite, chlorite, greenalite, and stilpnomelane. Mafic and ultramafic volcanic rocks (units 5 and 4, respectively) generally occur in the structural hanging wall of the ore zones. A massive quartzite, locally underlain by a basal polymictic conglomerate, structurally overlies the deposit host succession (Fig. 2). Minor mafic (unit 6) and intermediate (unit 7) volcanic rocks, respectively, consisting of chlorite and biotite schists, occur as conspicuous layers within the quartzite.

GEOCHEMISTRY OF PROTOLITHS

Rocks proximal to mineralized zones are strongly altered and their primary geochemical signatures (especially mobile major oxides and trace elements) are commonly obscured. Although visual recognition of the rock units allows for a preliminary classification, lithogeochemical data and more specifically least mobile elements such as Zr, Ti, Al, Y, Cr, Ni, Sc, V, and rare-earth elements (REE) are essential to further differentiate the subtle lithological variations, characterize distinct protoliths, and thus facilitates mapping of individual units. Lithogeochemical data and analysis of Janvier et al. (2015) are summarized herein.

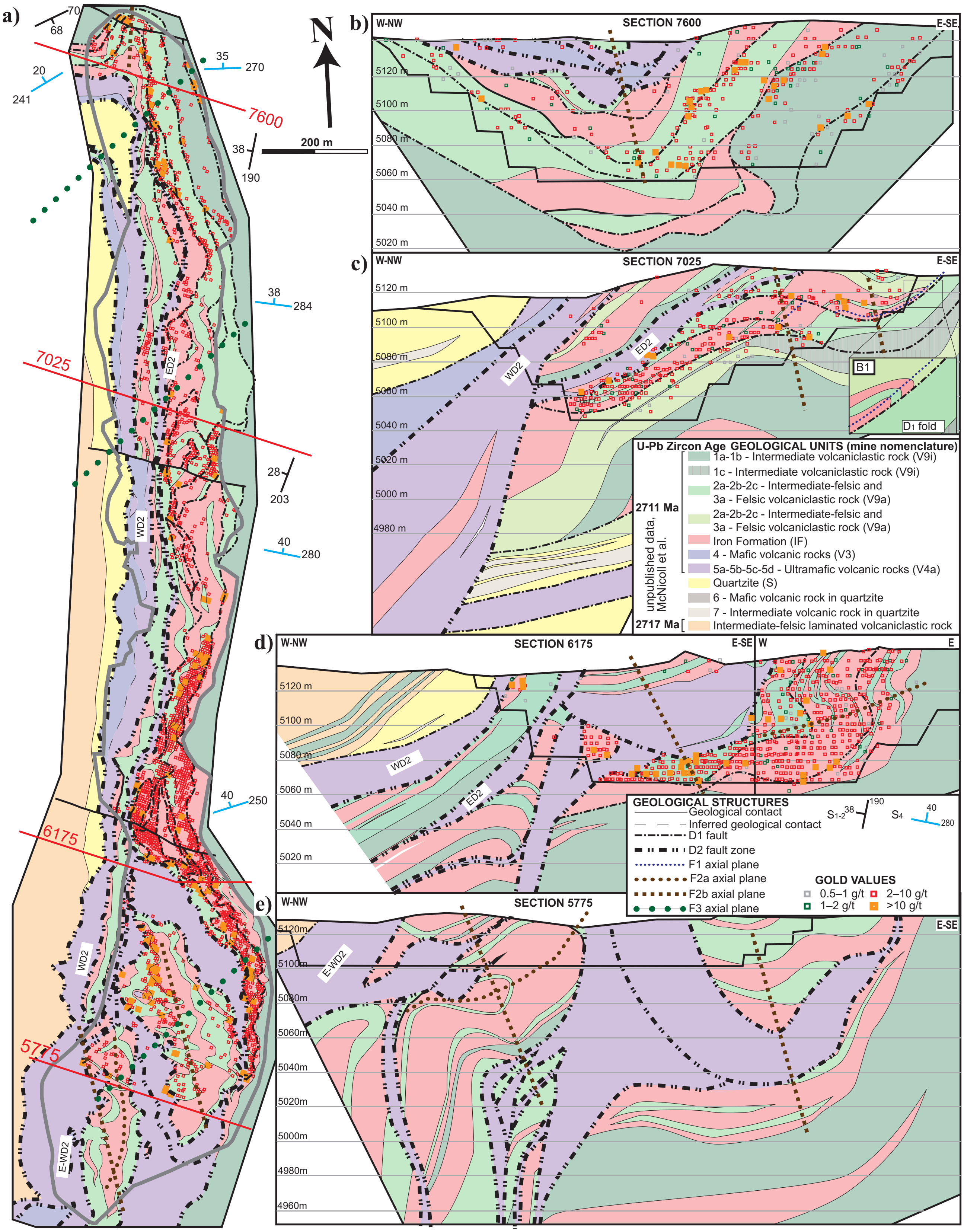

Figure 2. a) Geological map (based on drill sections, pit mapping, and geochemical characterization) of the Portage deposit (Meadowbank mine) at level 5102 m. Interpreted geology of sections **(b)** N7025, **(c)** N7600, **(d)** N5775, and **(e)** N6175 across the Portage deposit showing the complex fault imbrications and the distribution of gold. The gold values are from blast holes and are present inside the pit outline. Gold values are not available for section N5775. Mine-scale structural nomenclature modified from Pehrsson et al., 2013. U-Pb ages from Davis and Zaleski (1998) and McNicoll et al (unpublished data).

The Zr/TiO_2 versus Al_2O_3/TiO_2 binary diagram is useful to discriminate the main groups of volcanic rocks and various sub-units (Fig. 3a). Intermediate (unit 1: 1a, 1b, 1c) to felsic (unit 2: 2a, 2b, 2c), volcanic and/or volcaniclastic units yield andesitic and calc-alkaline compositions (Fig. 3b,c. Felsic volcaniclastic rocks (unit 3) yield trachyte and calc-alkaline compositions (Fig. 3b,c). Mafic (unit 4) and ultramafic units (unit 5) yield transitional to tholeiitic magmatic affinities (Fig. 3b) and a high-Fe basalt and basaltic komatiite compositions (Fig. 3d), respectively. Chondrite-normalized trace and rare-earth elements plots further help to differentiate units and subunits. Units 1 and 2 (Fig. 3e,f) have an arc-like signature with negative Nb, Ta, and Ti anomalies. Intermediate sub-units have elevated heavy-REE concentrations relative to intermediate to felsic sub-units (Fig. 3e,f). Mafic units yield flat REE patterns that range from 10 to 30 times chondritic compositions (Fig. 3g); whereas sub-units 5a, 5b, and 5c have generally lower REE values than mafic units (Fig. 3h), with depleted to enriched light-REE relative to heavy-REE. Unit 3 is distinct with much higher Zr/TiO_2 and Al_2O_3/TiO_2 ratios (Fig. 3a) and yield rhyodacitic to rhyolitic compositions (Fig. 3b) and a calc-alkaline affinity (Fig. 3c). Chondrite-normalized trace and REE plots for this unit show variable patterns with a moderate negative slope, and slightly negative Zr and strongly negative Ti anomalies (Fig. 3f).

STRUCTURE

The structural setting of Meadowbank deposit is highly complex and ore zones are strongly deformed (e.g. Sherlock et al., 2001a,b, 2004; Pehrsson et al., 2004, 2013; Janvier et al., 2013, 2015). Detailed mapping of the Portage and Goose open pits has delineated seven generations of structures defined on the basis of structural style, orientation, and relative crosscutting relationships. Each deformation increment is described below in apparent chronological order: 1) Along the eastern wall of the Portage open pit, a penetrative bedding-/layering-parallel schistosity, S_1, is generally south-trending and dips shallowly to moderately (~30°) to the west (Fig. 2a). The S_1 schistosity is associated with isoclinal folds (F_1). One of the F_1 folds, apparently east-verging, is mapped in the western part of the Portage open pit, as shown on section 7025 (Fig. 2c). 2) A large fault zone consisting of a series of discrete D_1 faults occurs in the Portage open pit causing the imbrication of volcaniclastic rocks, iron formation, and quartzite (Fig. 2). No reliable kinematic indicators have been identified for these faults. However, based on the interpreted section 7025 (Fig. 2c), the latter are apparently east-directed. The relative timing of such early faults is difficult to determine, but they are clearly folded and faulted by D_2 structures and are therefore termed D_1 faults (Fig. 2). 3) Tight to isoclinal F_{2a} folds with sub-horizontal south-trending axes occur in the southeastern part of the Portage open pit (Fig. 2a,e) and eastward, where asymmetric F_{2a} folds affect mineralized BIFs and intermediate to felsic rocks (Fig. 2d). Mesoscopic isoclinal F_{2a} folds have an apparent eastward vergence. An axial planar S_{2a} foliation is mostly developed along the limbs of F_{2a} folds, where it is coplanar to the S_1 schistosity and forms a composite S_{1-2} fabric (Fig. 4a). 4) A network of late D_2 fault zones is distinctively outlined by ultramafic rocks in the Portage open pit. Two of these, termed the western and eastern fault zones, are subparallel and mapped along parts of the western wall (Figs. 2, 4b). These structures, which cut D_1 faults and the ore zones, are affected by F_{2b}, F_3, and F_4 folds (Fig. 2). Although kinematic indicators are rare in volcanic units, some found in sheared ultramafic rocks suggest a down-to-the-west motion (inverted/folded thrust?). 5) North-trending upright gentle folds or undulations, termed F_{2b} folds herein, deform previous structures such as D_1 (Fig. 2a,c) or D_2 fault zones (Fig. 2e). Two late folding events are also differentiated by their vergence and wavelength. 6) In the northern part of the Portage open pit, the mine sequence turns abruptly to the west, affected by a shallow southwest-plunging, southeast-verging megascopic F_3 chevron-style synform, without a penetrative axial-planar fabric (Fig. 2a). Southward, along the long limb of this megascopic fold, minor F_3 folds occur in the Portage open pit, where they produce slight undulations of the lithological contacts and main fabric (Fig. 2). The structure of the southern part of the Portage open pit is dominated by a dome-and-basin pattern, resulting from the interference of F_3 and F_{2b} folds (Fig. 2). 7) D_4 deformation is characterized by mesoscopic shallowly to moderately inclined, south-verging, open to tight folds. The conspicuous axial-planar crenulation cleavage (S_4) is roughly west-trending and dips between 10 and 45° to the north (Fig. 2a).

ORE ZONES: MINERAL ASSEMBLAGES AND DISTRIBUTION

Banded Iron Formation-Hosted Gold

The bulk of the gold in the Meadowbank deposit is hosted in Algoma-type, banded magnetite-chert iron formations (BIF). Ore-bearing BIFs are intensely deformed, with pyrrhotite ±pyrite as the main ore-related minerals, together with lesser chalcopyrite and arsenopyrite. Grunerite is common in chert bands (Fig. 4c,d). In general, pyrrhotite/pyrite replace magnetite bands (Fig. 4c) and occur within high-strain zones (Fig. 4a) or as a transposed stockwork in magnetite and chert bands along with chlorite alteration (Fig. 4d). The gold-rich intersections (≥2 g/t) are often intensely deformed and primary layering of the host BIF is transposed or disrupted, forming dismembered masses of

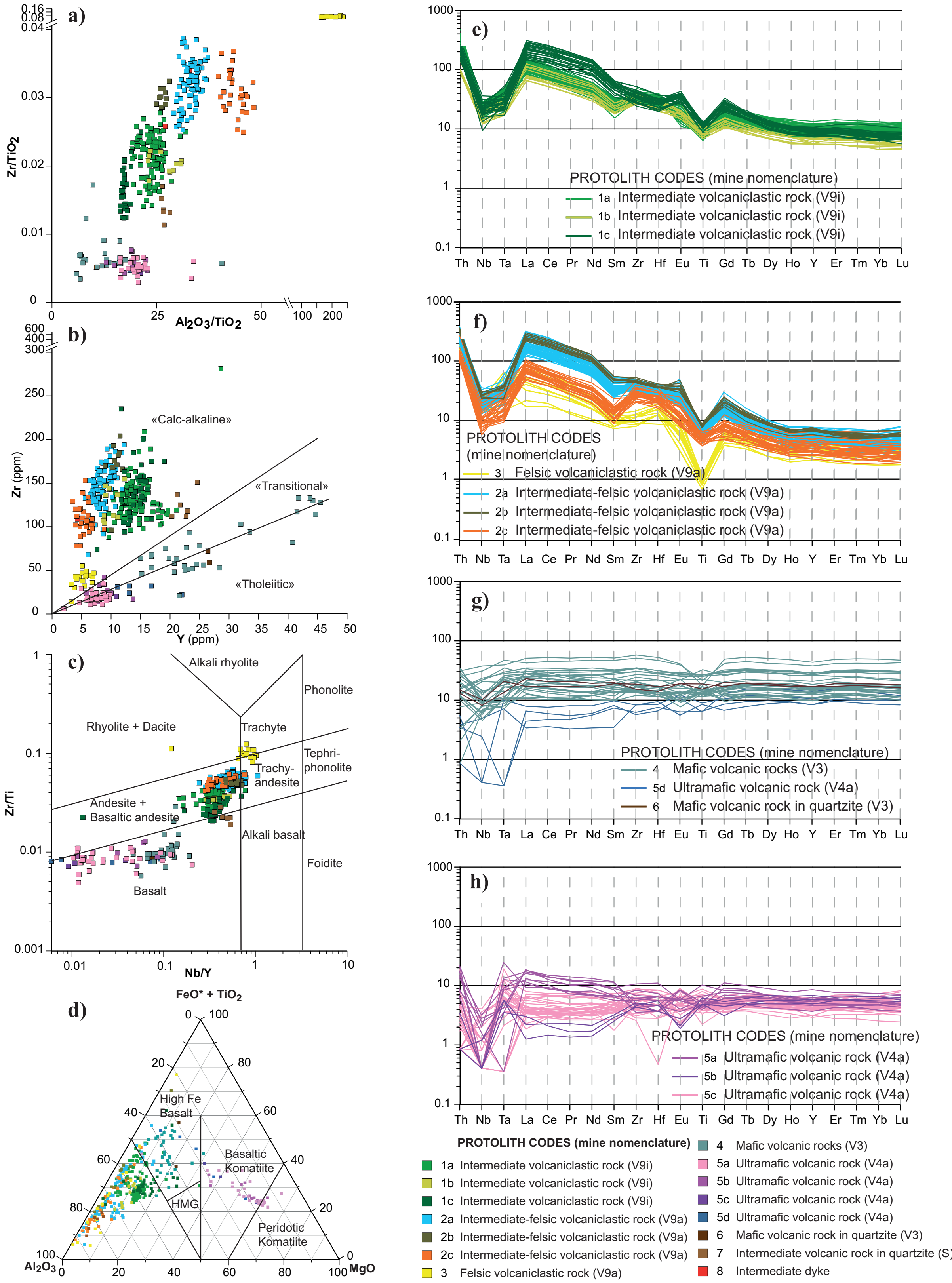

Figure 3. Geochemical diagrams for the volcanic and volcaniclastic rocks of the Meadowbank deposit area. **a)** Zr/TiO_2 versus Al_2O_3/TiO_2; **b)** Zr versus Y magmatic affinity diagram from MacLean and Barrett (1993); **c)** Zr/Ti versus Nb/Y classification diagram (Winchester and Floyd, 1977); **d)** AFM ternary diagram from Jensen (1976). Geochemical plots for volcanic and volcaniclastic rocks of the host rocks of the Meadowbank deposit. Abbreviation: HMG = high-magnesium tholeiite (basalt). **e)** C1 chondrite normalized (McDonough and Sun, 1995) multi-elements patterns for units 1a, 1b and 1c; **f)** units 2a, 2b, 2c, and 3; **g)** units 4, 5d, and 6; and **h)** units 5a, 5b, and 5c.

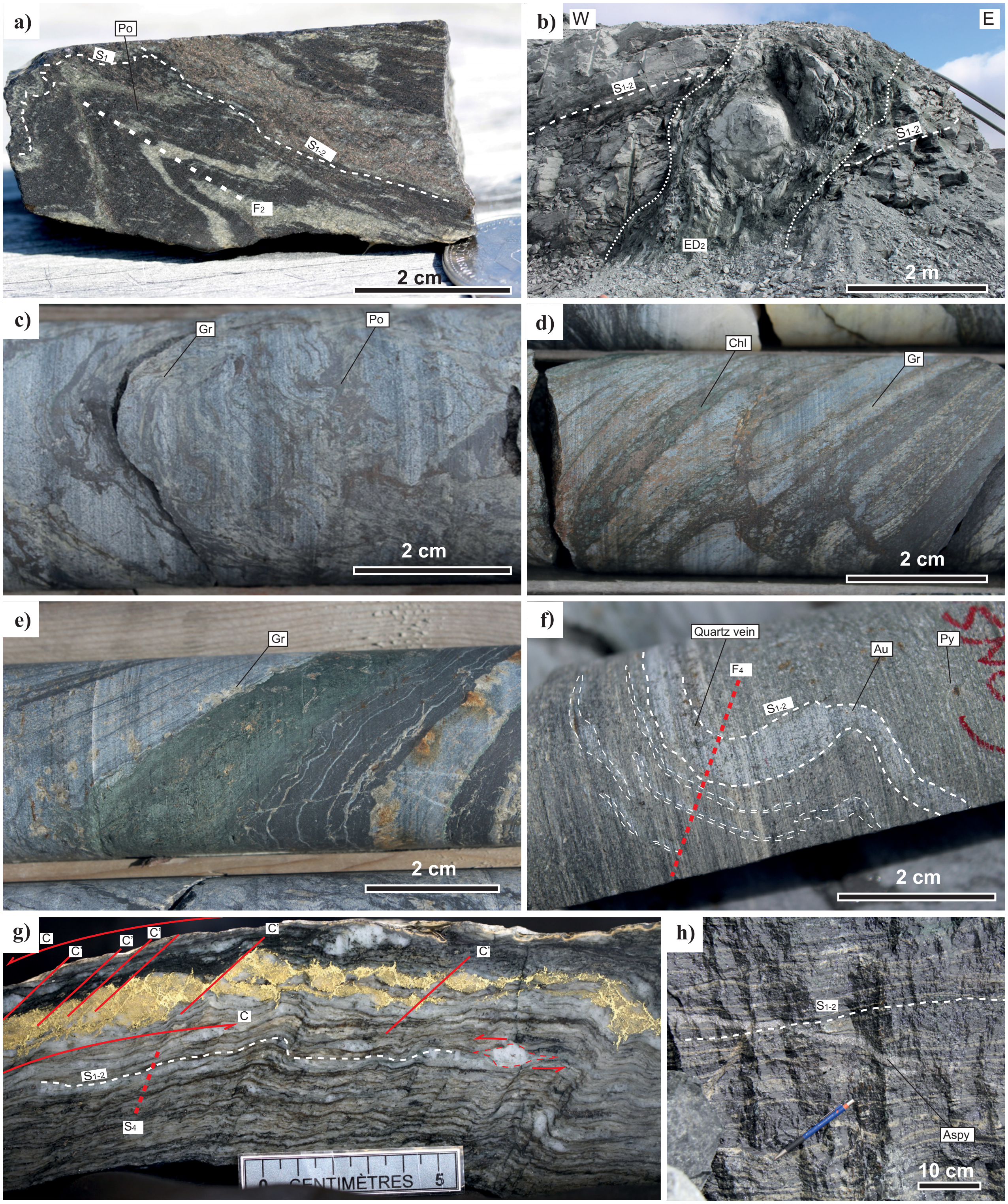

Figure 4. Representative photographs of mineralized and barren banded iron formations (BIFs) and volcaniclastic rocks with associated mineral assemblages of the Meadowbank deposit. **a)** BIF with pyrrhotite (Po) replacing magnetite layers along the S_1 fabric and remobilized along a sheared F_2 fold limb. **b)** The Eastern D_2 fault zone (ED2) marked by ultramafic rocks cutting the composite $S_{1\text{-}2}$ fabric in the volcaniclastic rocks. **c)** Mineralized and strongly deformed BIF; note the thin disseminated grunerite (Gr) where pyrrhotite (Po) replaces magnetite. **d)** Transposed pyrrhotite and pyrite stockwork in BIF-chert layers with minor chlorite (Chl) alteration. **e)** Barren BIF with chlorite-rich bands and acicular grunerite at the margins of Fe-oxide bands. **f)** Intermediate to felsic volcaniclastic rock with a pyrite-chlorite- muscovite assemblage adjacent to a quartz-gold vein deformed by F_4 folding. **g)** Felsic schist showing the composite $S_{1\text{-}2}$ fabric and transposed (C: shear plane) and boudinaged (C': synthetic riedel or secondary shear plane) gold-quartz veins, affected by the S_4 crenulation cleavage). **h)** Arsenopyrite (Aspy) vein (arrow) cutting the BIF layering and affected by the $S_{1\text{-}2}$ fabric. (Mine-scale structural nomenclature).

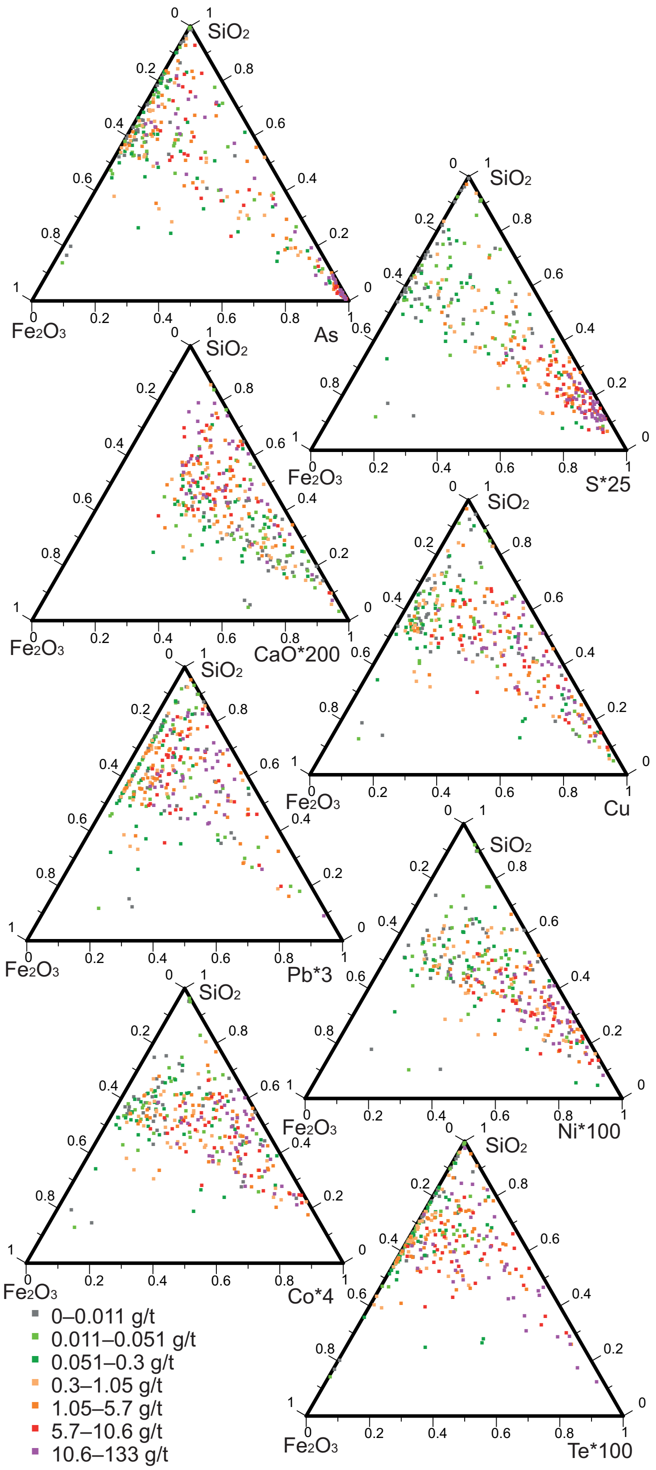

Figure 5. SiO_2-Fe_2O_3-X ternary diagrams representing the relative abundance of various elements versus gold grade of iron formation samples.

quartz, pyrrhotite, and relict magnetite (Fig. 4a,c). Arsenic, S, Cu, Pb, Ni, Co, and Te are anomalous in auriferous BIF, whereas Ca seems to have been leached (Fig. 5). Barren BIFs are much less deformed and have dark green chlorite-rich layers and coarse-grained acicular grunerite (Fig. 4e).

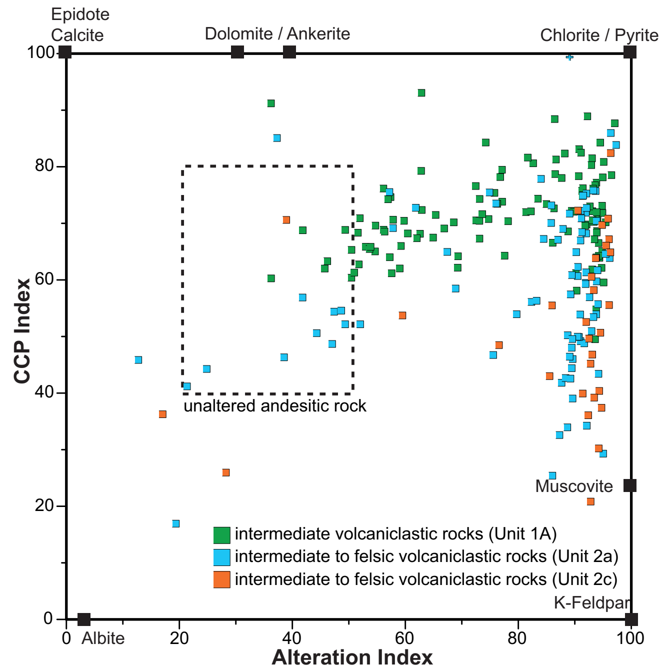

Figure 6. AI-CCPI alteration box plot illustrating chlorite/pyrite and muscovite alteration poles. AI (Ishikawa alteration index) = $100(MgO+K_2O)/(MgO+K_2O+CaO+Na_2O)$ (Ishikawa et al., 1976); CCPI (chlorite-carbonate-pyrite index) = $100(FeO+MgO)/(FeO+MgO+Na_2O+K_2O)$ (modified from Large et al., 2001). Such a diagram has been principally developed for Kuroko-style volcanogenic massive sulphide deposits, and is used herein as a first-order analysis of our data.

Volcaniclastic Rock-Hosted Gold

A second style of mineralization consists of gold-bearing quartz-pyrrhotite ±pyrite veins hosted by intermediate to felsic volcaniclastic rocks (Fig. 4f). This style of mineralization is locally associated with spectacular high-grade ore (Fig. 4g). Auriferous veins are transposed, sheared, and boudinaged sub-parallel to the composite $S_{1\text{-}2}$ schistosity and pre-date the S_4 fabric (Fig. 4f). Disseminated pyrite commonly occurs in the selvages of these veins (Fig. 4f), which are marked by metre-scale chlorite-muscovite alteration halos. An alteration boxplot diagram (Fig. 6; Large et al., 2001) supports this observation and shows that altered samples plot towards the chlorite/pyrite and muscovite poles. Following the single precursor method of MacLean and Barrett (1993), mass changes resulting from alteration were calculated using protoliths that were selected based on low loss-on-ignition values and petrographic observations. Intermediate (subunit 1a) and intermediate to felsic rock (subunit 2a) samples show a loss in Na_2O and CaO (~75–100%), reflecting a strong feldspar destruction, and a gain in K_2O (~25–75%), attributed to the muscovite alteration (Fig. 7). Such mass gain of 0.89 to 5.41 wt% K_2O and loss of 0.67 to 3.66 wt% Na_2O are predominantly observed in subunit 2a, which may be explained by its spatial asso-

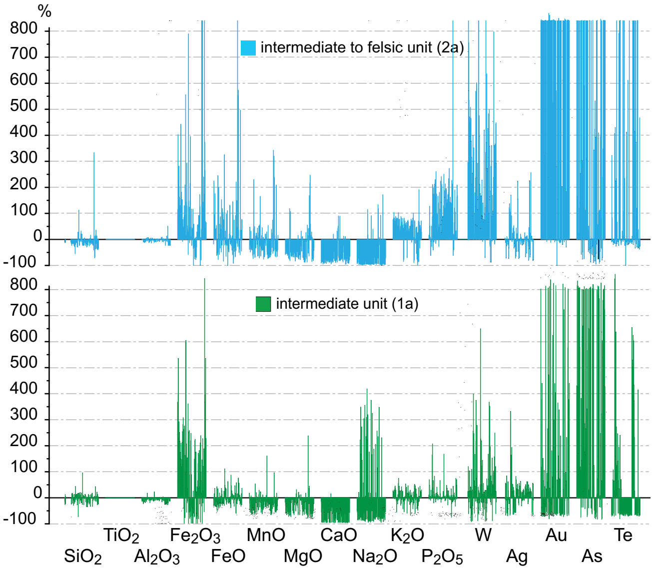

Figure 7. Mass balance diagram (based on the method of MacLean and Barrett, 1993) showing the gains and losses (in percentage) of major elements for intermediate and intermediate to felsic rock samples compared to least altered samples.

ciation with the ore zone (Fig. 8). The mass balance diagram also shows strong gains in Fe_2O_3, P_2O_5, W, As, and Te (Fig. 7). Although some disseminated calcite occurs in subunit 1c, no carbonate alteration is associated with the Portage-Goose deposit. Metamorphic grade transitions from greenschist facies at Portage to amphibolite facies at Goose, which is reflected by a change in the dominant hydrothermal mineral alteration assemblage (i.e. chlorite-muscovite vs. biotite± Fe-Mg amphibole ±garnet; Pehrsson et al., 2004; Sherlock et al., 2004).

Gold Distribution

There are important spatial relationships between the ore zones and some of the earliest structures of the deposit. In the southern part of the Portage open pit (sections 5775 and 6175; Fig. 2a,d,e), the ore zones are hosted in iron formation and occur along D_1 faults and/or proximal to D_2 fault/shear zones. Northward in the Portage open pit, gold mineralization is also hosted, in part, by volcaniclastic rocks and occurs along several subparallel planar ore zones (Fig. 2a,b,c). These ore zones are discordant to lithological contacts, locally coincide with truncations of units, and are thus interpreted to mark discrete D_1 faults. The concentration of sulphides along sheared F_{2a} fold limbs (Fig. 4a) suggests that part of the ore was remobilized or introduced during early- to syn-D_2 deformation. Late idioblastic arsenopyrite veins pre-date the $S_{1\text{-}2}$ fabric and also suggest an early- to syn-D_2 mineralizing event (Fig. 4h). Preliminary Re-Os dating of this arsenopyrite gave an age of ca. 1899 Ma (Janvier et al., in prep.).

DISCUSSION

The analysis of the «immobile elements» has allowed for the identification of several, previously undifferentiated, distinctive volcanic subunits. Three intermediate subunits (i.e. 1a, 1b and 1c), three intermediate to felsic subunits (i.e. 2a, 2b and 2c), one felsic unit (i.e. 3), one mafic unit (i.e. 4), and four ultramafic subunits (i.e. 5a, 5b, 5c and 5d) have been identified. This detailed subdivision has allowed for better definition of the lithostratigraphic and structural settings of the Portage-Goose deposit. Characterization of the primary composition of the host units of the Portage-Goose deposit have allowed us to identify and quantify a potassic alteration proximal to the ore zones that is substantiated by an abundance of muscovite in the volcanoclastic rocks. Such an alteration is typical of lode-gold deposits (Poulsen et al., 2000). The mine-scale protoliths defined herein correlate with those established regionally (Zaleski et al., 1999b; Pehrsson et al., 2013), despite the use of different data sets. As such, regional protolith determination can be used as a regional exploration tool to outline the specific prospective stratigraphic horizons and trace key geological structures.

The various generations of structures defined in the Meadowbank deposit area can be correlated with the regional deformation phases of Pehrsson et al. (2013), although some apparent structural vergence or crosscutting relationships appear to be contradictory. D_1 fabrics (schistosity, isoclinal folds and faults) correlate with the D_{P1} deformation phase of Pehrsson et al. (2013). However, the apparent eastward vergence of the discrete D_1 faults mapped at the Portage deposit contrasts with the overall south vergence of the regional D_{P1} deformation (Pehrsson et al., 2013). Incremental deposit-scale D_2 structures, comprising D_{2a} folds, D_2 fault zones, and D_{2b} gentle folds, are all interpreted to be associated with the regional D_{P2} deformation (Pehrsson et al., 2013). The actual dip and apparent down-to-the-west motion of D_2 fault zones are interpreted as resulting from D_3 folding and are otherwise compatible with the regional northwest-directed D_{P2} thrusting documented by Pehrsson et al. (2013). The two late phases of folding (D_3 and D_4) are also correlated with the regional D_{P3} and D_{P4} folding events (Pehrsson et al., 2013), however, their relative timing established by deposit-scale crosscutting relationships appears to be contradictory and reversed (i.e. deposit-scale F_3 and F_4 folds correspond to the regional F_{P4} and F_{P3} folds, respectively). The consistent orientation of S_4 crenulation cleavage at the mine scale suggests that D_4 deformation represents the youngest folding phase.

Establishing the relationships and controls between structural geology and gold mineralization is a key aspect of the present study. Our study indicates that

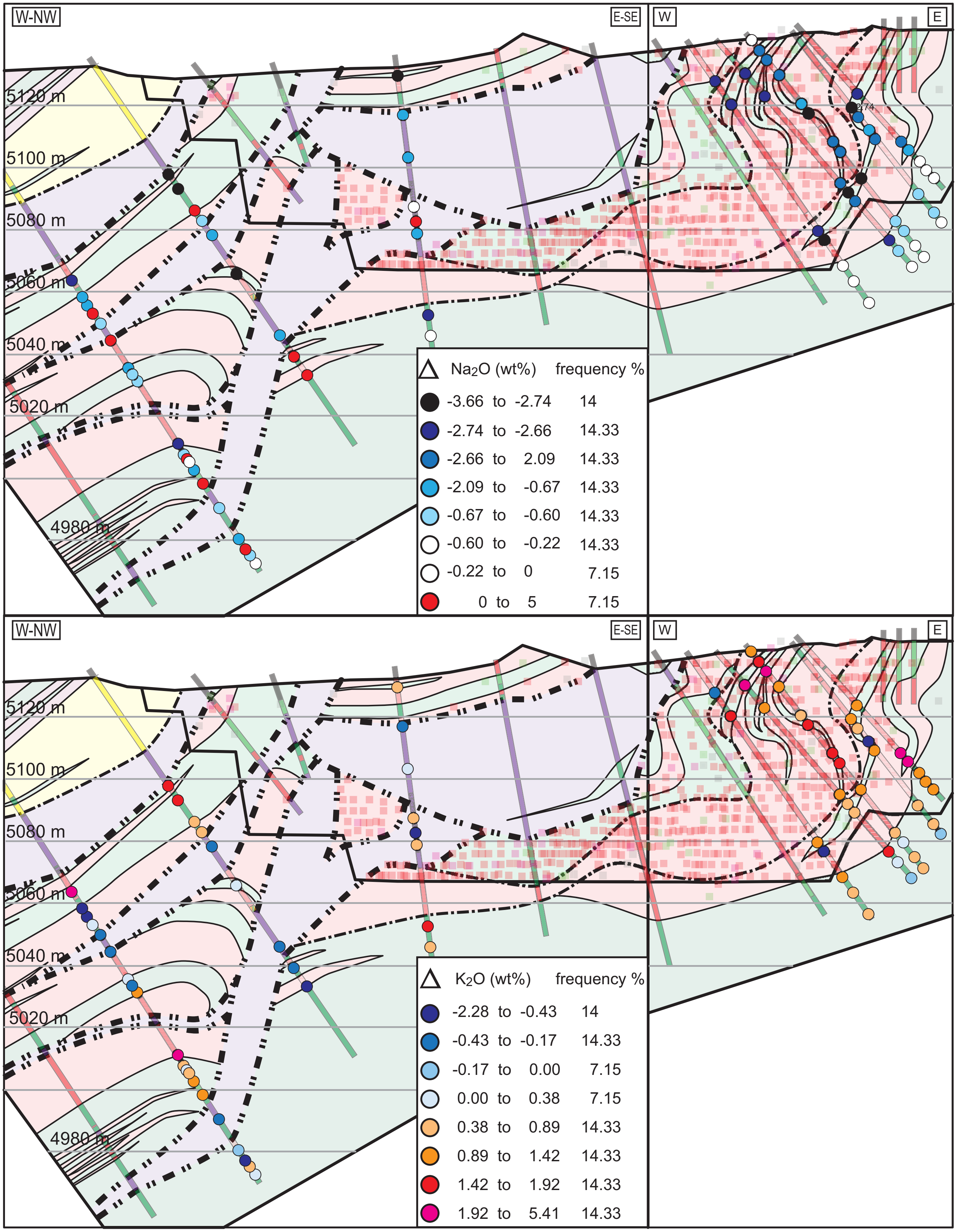

Figure 8. Calculated mass changes in Na_2O and K_2O in absolute weight percent (based on the method of MacLean and Barrett, 1993) of samples of drill section 6175

lithological (BIF) and structural traps (network of D_1 and D_2 fault zones) have clearly exerted a control on the location and geometry of the gold-rich ore at Meadowbank. Competence contrasts between BIF and volcaniclastic and ultramafic rocks contributed to strain localization and/or partitioning and fluid circulation in the highly reactive BIF, allowing gold to precipitate. Previous research (e.g. Armitage et al., 1996; Sherlock et al., 2004) has proposed that gold was introduced during the regional D_{P2} deformation at ca. 1.83 Ga. We propose that gold mineralization occurred prior to, or very early during D_{P2} based on the following reasoning: 1) the occurrence of transposed-boudinaged (remobilized) high-grade gold-quartz veins into the composite S_{1-2} foliation (Fig. 4g) suggest that gold-quartz veins were introduced either during D_1 or early during D_2; 2) D_2 fault zones cut planar ore zones (D_1 faults) affected by composite S_{1-2} fabric (Figs. 2c, 4b); 3) S_1-foliated magnetite layers (S_0) are replaced by pyrrhotite and are folded by mesoscopic F_2 folds (Fig. 4a); 4) at the pit-scale, gold is spatially associated with D_1 faults (Fig. 2), which are folded by both sets of F_2 folds (Fig. 2c,e); and 5) a preliminary Re-Os age of an auriferous arsenopyrite vein cutting the S_{1-2}-foliated chert-magnetite layering yielded an age of ca. 1899 Ma, which is contemporaneous with the older published age constraints for D_{P1} and D_{P2} (i.e. 1.91–1.83 Ga; Pehrsson et al., 2013; Fig. 4h).

IMPLICATIONS FOR EXPLORATION

Access to open-pit workings, new outcrops, exploration and delineation drilling, and mining data, coupled with in-depth geochemical characterization of the Meadowbank deposit host rocks provides new constraints on the lithostratigraphic setting and structure of the Meadowbank deposit. The bulk of the gold mineralization in the Meadowbank deposit is accompanied by pyrrhotite, grunerite, and minor chlorite, and hosted in strongly deformed BIF, within or adjacent to fault/shear zones. A significant amount of the gold also occurs in quartz veins in adjacent muscovite-altered volcaniclastic rocks, in association with disseminated pyrite, muscovite, and chlorite. Elevated P_2O_5, W, As, Cu, Pb, Ni, Co, and Te represent the hydrothermal footprint of the Meadowbank auriferous system. Contrary to other shear-zone-related gold deposits, there is no significant carbonate alteration at Meadowbank.

Hitherto undocumented fault zones (D_1 and D_2) represent important controls on the geometry of the gold at the ore-zone to deposit scales. Crosscutting relationships and preliminary Re-Os arsenopyrite ages suggest that gold mineralization occurred prior to the peak of D_{P2} deformation. We propose that D_{P1} fault zones played a major control on the actual ore distribution and probably the genesis of the deposit. Deposit- and regional-scale mapping, lithogeochemistry, and U-Pb zircon geochronology indicate that the Meadowbank BIF-hosted deposit is located at or very near the boundary between two petrographically and geochemically distinct rock packages (2711 Ma and 2717 Ma; Fig. 1; McNicoll et al (unpublished data)), which are separated by long-lived fault zones (D_{P1}) (or reactivated Archean structures?). Such an interpretation may explain why gold is confined to the central BIF (Figs. 1, 2). Identifying and following such early structures may constitute regional exploration vectors. Research results presented herein suggest that some of the gold mineralization processes are older than previously thought, which may have implications for exploration strategies in Archean sequences affected by younger Proterozoic deformation.

FUTURE WORK

On-going work at Meadowbank aims to 1) better constraining the relative and absolute timing of the ore-forming events and the geochemical and mineralogical signatures of the gold-bearing hydrothermal event(s); and 2) extrapolate the structural model for the Meadowbank deposit at the scale of the Woodburn Lake Group in order to identify and follow structures or favourable geological settings for gold mineralization.

ACKNOWLEDGEMENTS

This contribution emanates mainly from the Ph.D. thesis research of lead author (V. Janvier) at the Institut national de la recherche scientifique (INRS-ETE), as part of the Targeted Geoscience Initiative 4 (Lode Gold project) of Natural Resources Canada. We thank Agnico Eagle Mines Ltd for access to the property, to drill cores and various databases, and for chartered transport and accommodation during fieldwork. The staffs of the AEM Meadowbank and Exploration divisions are acknowledged for their time, full operational and scientific support and interest in this project. We thank Christopher Lawley for his constructive comments and suggestions.

REFERENCES

Armitage, A.E., James, R.S., and Goff, S.P., 1996. Gold mineralization in Archean banded iron formation, Third Portage Lake area, Northwest Territories, Canada; Exploration and Mining Geology, v. 5, p. 1–15.

Ashton, K.E., 1988. Precambrian geology of the southeastern Amer Lake area (66H/1), near Baker Lake, N.W.T.: a study of the Woodburn Lake Group, an Archean orthoquartzite-bearing sequence in the Churchill structural province; Ph.D. thesis, Queen's University, Kingston, Ontario, 335 p.

Berman, R.G., Sanborn-Barrie, M., Stern, R.A., and Carson, C.J., 2005. Tectonometamorphism at ca. 2.35 and 1.85 Ga in the Rae domain, western Churchill Province, Nunavut, Canada: insights from structural, metamorphic and in situ geochronological analysis of the southwestern Committee Bay Belt; The Canadian Mineralogist, v. 43, p. 409–442.

Berman, R.G., Davis, W.J., and Pehrsson, S., 2007. Collisional Snowbird tectonic zone resurrected: Growth of Laurentia during the 1.9 Ga accretionary phase of the Hudsonian orogeny; Geology, v. 35, p. 911–914.

Castonguay, S., Janvier, V., Mercier-Langevin, P., Dubé, B., McNicoll, V., Malo, M., Pehrsson, S., and Bécu, V., 2012. Recognizing optimum banded-iron formation-hosted gold environments in ancient, deformed and metamorphosed terranes: preliminary results from the Meadowbank deposit, Nunavut, *In:* Program with Abstracts; 40th Annual Yellowknife Geoscience Forum, Yellowknife, Northwest Territories.

Castonguay, S., Janvier, V., Mercier-Langevin, P., Dubé, B., McNicoll, V., Malo, M., Pehrsson, S., and Bécu, V., 2013. Recognizing optimum banded iron formation (BIF)-hosted gold environments: preliminary results from the Meadowbank deposit, *In:* Program with Abstracts 2013; Nunavut Mining Symposium, Iqaluit, Nunavut.

Davis, W.J. and Zaleski, E., 1998. Geochronological investigations of the Woodburn Lake group, western Churchill Province, Northwest Territories: preliminary results, *In:* Radiogenic Age and Isotopic Studies, Report 11; Geological Survey of Canada, Current Research no. 1998-F, p. 89–97

Dupuis, C., Mercier-Langevin, P., McNicoll, Janvier, V., Dubé, B., Castonguay, S., de Chavigny, B., Pehrsson, S., and Côté-Mantha, O., 2014. The Vault gold deposit, Meadowbank area, Nunavut: Preliminary results on the nature and timing of mineralization, *In:* Program with Abstracts; Geological Association of Canada – Mineralogical Association of Canada annual joint meeting, Fredericton, New Brunswick, v. 37, p. 81.

Gourcerol, B., Thurston, P.C., Kontak, D.J., and Côté-Mantha, O., 2014. Interpretations and implications of preliminary LA ICP-MS analysis of chert for the origin of geochemical signatures in banded iron-formations from the Meadowbank gold deposit, western Churchill Province, Nunavut; Geological Survey of Canada, Current Research 2014-1, 22 p.

Gourcerol, B., Thurston, P.C., Kontak, D.J., Côté-Mantha, O. and Biczok, J., 2015. Depositional setting of Algoma-type banded iron formation from the Meadowbank, Meliadine and Musselwhite gold deposits, *In:* Targeted Geoscience Initiative 4: Contributions to the understanding of Precambrian lode gold deposits and implications for exploration, (ed.) B. Dubé and P. Mercier-Langevin; Geological Survey of Canada, Open File 7852, p. 55–68.

Henderson, J.R., Henderson, M.N., Pryer, L.L., and Cresswell, R.G., 1991. Geology of the Whitehills-Tehek area, District of Keewatin: an Archean supracrustal belt with iron formation-hosted gold mineralization in the central Churchill Province, *In:* Current Research, Part C; Geological Survey of Canada, Paper 91-01C, p. 149–156.

Hoffman, P.F., 1989. Precambrian geology and tectonic history of North America In: The Geology of North America – An Overview: The Geology of North America, Part A; Geological Society of America, p. 447–512.

Hrabi, R.B., Barclay, W.A., Fleming, D., and Alexander, R.B., 2003. Structural evolution of the Woodburn Lake group in the area of the Meadowbank gold deposit, Nunavut; Geological Survey of Canada, Current Research 2003-C27, p. 10.

Ishikawa, Y., Sawaguchi, T., Iwaya, S., and Horiuchi, M., 1976. Delineation of prospecting targets for Kuroko deposits based on modes of volcanism of underlying dacite and alteration halos; Mining Geology, v. 26, p. 105–117 (in Japanese with English abstract).

Janvier, V., Castonguay, S., Mercier-Langevin, P., Dubé, B., McNicoll, V., Malo, M., Pehrsson, S.J., and Bécu, V., 2013. Recognizing optimum banded-iron formation-hosted gold environments in ancient, deformed and metamorphosed terranes: Preliminary results from the Meadowbank deposit, Nunavut, Canada; Geological Survey of Canada, Open File 7407. doi:10.4095/292589

Janvier, V., Castonguay, S., Mercier-Langevin, P., Dubé, B., McNicoll, V., Pehrsson, S., Malo, M., De Chavigny, B., and Côté-Mantha, O., 2015. Geology of the Portage deposit, Meadowbank gold mine, Churchill Province, Nunavut; Geological Survey of Canada, Current Research 2015-2, 18 p.

Jensen, L.S., 1976. A new cation plot for classifying subalcalic volcanic rocks; Ontario Division of Mines, Miscellaneous Paper 66, 21 p.

Large, R.R., Gemmell, J.B., Paulick, H., and Huston, D.L., 2001. The alteration box plot: A simple approach to understanding the relationship between alteration mineralogy and lithogeochemistry associated with volcanic-hosted massive sulfide deposits; Economic Geology, v. 96, p. 957–971.

MacLean, W.H. and Barrett, T.J., 1993. Lithogeochemical techniques using immobile elements; Journal of Geochemical Exploration, v. 48, p. 109–133.

Pehrsson, S.J., Wilkinson, L., and Zaleski, E., 2004. Geology of the Meadowbank gold deposit area, Nunavut: Geological Survey of Canada, Open File 4269, scale 1:20,000.

Pehrsson, S.J., Berman, R.G., and Davis, W.J., 2013. Paleoproterozoic orogenesis during Nuna aggregation: A case study of reworking of the Rae craton, Woodburn Lake, Nunavut; Precambrian Research, v. 232, p. 167–188.

Poulsen, K.H., Robert, F., and Dubé, B., 2000. Geological classification of Canadian gold deposits; Geological Survey of Canada, Bulletin 540, 106 p.

Sherlock, R.L., Alexander, R.B., March, R., Kellner, J., and Barclay, W.A., 2001a. Geological setting of the Meadowbank iron-formation-hosted gold deposits, Nunavut; Geological Survey of Canada, Current Research 2001-C11, 10 p.

Sherlock, R., Alexander, B., March, R., and Kellner, J., 2001b. Geologic setting of the Meadowbank iron formation hosted gold deposits; Geological Survey of Canada, Open file 3149, scale 1:10,000.

Sherlock, R., Pehrsson, S.J., Logan, A.V., Hrabi, R.B., and Davis, W.J., 2004. Geological Setting of the Meadowbank Gold Deposits, Woodburn Lake Group, Nunavut; Exploration and Mining Geology, v. 13, p. 67–107.

Skulski, T., Sandeman, H., Sanborn-Barrie, M., MacHattie, T., Young, M., Carson, C., Berman, R., Brown, N., Rayner, D., Pangapko, D., Byrne, D., and Deyell, C., 2003. Bedrock geology of the Ellice Hills map area and new constraints on the regional geology of the Committee Bay area, Nunavut; Geological Survey of Canada, Paper 2003-C22, 11 p.

Winchester, J.A. and Floyd, P.A., 1977. Geochemical discrimination of different magma series and their differentiation products using immobile elements; Chemical Geology, v. 20, p. 325–343.

Zaleski, E., Henderson, J.R., Corrigan, D., Jenner, G.A., Kjarsgaard, B.A., and Kerswill, J.A., 1997. Preliminary results of mapping and structural interpretation from the Woodburn project, western Churchill Province, Northwest Territories, *In:* 1996 Exploration Overview; Northwest Territories Geoscience Office, p. 3.43–3.44.

Zaleski, E., Duke, N., L'Heureux, R., and Wilkinson, L., 1999a. Geology, Woodburn Lake group, Amarulik Lake to Tehek Lake, Kivalliq Region, Nunavut; Geological Survey of Canada, Open File 3743, scale 1:50,000.

Zaleski, E., L'Heureux, R., Duke, N., and Wilkinson, L., 1999b. Komatiites and felsic volcanic rocks overlain by quartzite, Woodburn Lake group, Meadowbank River area, western

Churchill Province, Northwest Territories (Nunavut); Geological Survey of Canada, Current Research 1999-C, p. 9–18.

Zaleski, E., Davis, W.J., and Sandeman, H.A., 2001. Continental extension, mantle magmas and basement/ cover relationships, In: Extended Abstracts; Fourth International Archaean Symposium, Perth, Australia, p. 374–376.

Zaleski, E., Pehrsson, S., and Kerswill, J.A., 2003. Geology, Half Way Hills and Whitehills Lake area, Nunavut; Geological Survey of Canada, Map 1234A, scale 1:50,000.